Road Detection Using Fisheye Camera and Laser Range Finder

Yong Fang, Cindy Cappelle, and Yassine Ruichek

IRTES-SET, UTBM, 90010 Belfort Cedex, France

Abstract. Road detection is a significant task for the development of intelligent vehicles as well as advanced driver assistance systems (ADAS). For the past decade, many methods have been proposed. Among these approaches, one of them uses log-chromaticity space based illumination invariant grayscale image. However, errors in road detection could occur due to over saturation or under saturation, especially in weak lighting situations. In this paper, a new approach is proposed. It combines fisheye image information (in log-chromaticity space and in Lab color space) and laser range finder (LRF) measurements. Firstly, road is coarsely detected by a classifier based on the histogram of the illumination invariant grayscale image and a predefined road area. This fisheye image based coarse road detection is then faced to LRF measurements in order to detect eventual conflicts. Possible errors in coarse road detection can then be highlighted. Finally, in case of detected conflicts, a refined process based on Lab color space is carried out to rule out the errors. Experimental results based on real road scenes show the effectiveness of the proposed method.

Keywords: Road detection, Illumination invariant, Lab space, LRF.

1 Introduction

For autonomous vehicles and Advanced Driver Assistance Systems (ADAS), an important task is to keep the vehicle traveling in a safe region and prevent collisions. To meet that requirement, the vehicle has to perceive the structure of the environment around itself. The free road surface ahead of the vehicle has then to be detected. In addition, a robust effective road detection system also plays an important role in higher other tasks such as vehicle and pedestrian detection. The derived free road space can effectively provide a significant contextual information to reduce the region-of-interest for searching targets (cars,pedestians,...).

Road detection has been widely studied for past several years and many approaches have been proposed. According to the used equipments, methods can be categorized into three types:1)Approaches based on LRF, 2)Approaches based on camera, 3)Approaches based on both LRF and camera. In papers [1] and [2], the authors proposed approaches based on 3D LRF data. The road information is segmented from points cloud. The advantage of LRF is that it can provide reliable range measurements that are not likely affected by the illumination.

A. Elmoataz et al. (Eds.): ICISP 2014, LNCS 8509, pp. 495–502, 2014.

However, a limitation of this device is that it can't offer visual information, for example, traffic signals and object appearance. Yet, in many applications, such as object recognition and tracking, visual information is crucial for autonomous vehicle.

Compared to LRF, camera can offer substantive visual information in favor to the recognition of on-road objects and traffic signals. Generally, road detection based on vision is a challenging work for autonomous vehicle in outdoor scenario due to the background changement with vehicle traveling and the presence of many moving objects on the road whose movements are hard to predict. Therefore, a variety of vision-based approaches have been developed by researchers. In papers [3] and [4], stereo vision permits to compute the disparity map used to acquire the road information. Both two methods need to find features correspondence to calculate disparity map. False matching will lead to false detection. In paper [5], a mixture of Gaussians in RGB color space and a Gaussian distribution are used for road modeling. But it is hard to decide the proper number of Gaussians to use.

In our work, we aim at performing road detection using a monocular camera with fisheye lens and a 2D LRF. Compared to classic lens, fisheye lens has greater FOV providing more information about the scene. But the disadvantage is the great distortion appearing in the images. Therefore, we propose to use color space as feature space. In paper [6], the authors prove that the log-chromaticity based illumination invariant grayscale image is more suitable than HSI (hue, saturation, and intensity) (as done in paper [7]) for road detection. However, in our research, we notice that using only illumination invariant image can cause over saturation problem or under saturation problem in some cases such as cloudy situation. So, in this paper, a novel approach combining log-chromaticity space (as in paper [6]), Lab space [8] and LRF information is proposed. Firstly, the road is coarsely detected by a classifier. Then a validation step using LRF measurements is applied to the coarse road detection results to check if errors seem to occur. A refined processing based on lab color space information is applied to correct such possible errors. Otherwise, the coarse road detection results output directly.

The rest of the paper is organized as follows: Section 2 describes the coarse road detection based on illumination invariant image. Section 3 introduces how Lab color feature and LRF are used to refine the coarse road detection results. Section 4 shows real data experimental results and compares results of the proposed approach against illumination invariant based algorithm [6]. Conclusions are given in section 5.

2 Coarse Road Detection Based on Illumination Invariant Image

Our approach is based on fisheye image whose middle part is the context of the captured traffic scene and the remaining part is useless black area (see Fig.1(a)). The useless area, having side effect on solving illumination invariant grayscale image, is firstly removed (see Fig.1(b)). Then, the illumination invariant grayscale

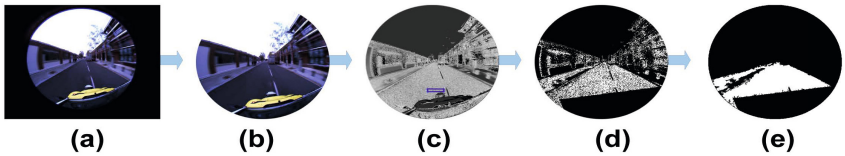

Fig. 1. (a) Fisheye image (b) The context part of fisheye image (c) The illumination invariant grayscale image of the context part of fisheye image (d) The classification result. To simplify computation, a fixed rectangle area containing the front part of the vehicle is treated as non-road by default (d) The coarse road detection result

image (see Fig.1(c)) is computed by mapping the context part from RGB to log-chromaticity space introduced by Finlayson et al.[9]. The "road" pixels are identified by a classifier based on the normalized histogram of the illumination invariant grayscale image and a predefined road area in this image. As in paper [10], the predefined road area is a fixed small region in front of vehicle in each illumination invariant grayscale image. S_r indicates the fixed road area (represented as a blue rectangle in Fig.1(c)). G_{rmin} and G_{rmax} are respectively the minimum and maximum gray level of illumination invariant image in S_r area. Let denote G_i the gray level of i-th pixel in illumination invariant image and λ_i the probability of this i-th pixel in the normalized histogram of illumination invariant image. The classifier categorizing the illumination invariant grayscale image into two classes "road" and "non-road" is built on the following rules:

$$\begin{cases} G_{rmin} < G_i < G_{rmax} (i = 1, 2, ..., N) \\ \lambda_i > \lambda_f (\lambda_f > 0) \end{cases} \tag{1}$$

where λ_f is a threshold which is set to 0.25 and N is the number of pixels in the image. If the above two conditions are satisfied, the pixel is identified as road and its value is set to 1. Otherwise, the i-th pixel is identified as non-road and its value is set to 0. However, many scattered pieces of road pixels are produced by the classification operation (see Fig.1(d)). To form a complete road binary image, a flood-fill operation and connected-component algorithm are applied to the binary image obtained by the classification algorithm. The flood-fill operation is based on morphology and is used to fill holes in the image. The connected-component algorithm is used to rule out the pixels which are not connected to the region including the predefined road area S_r in 8-connected neighborhood. An example of obtained coarse road binary image is given in Fig.1(e).

3 Refined Road Detection

3.1 Coherence Checking between Coarse Road Detection and LRF Measurements

After the previous described steps, there may exist some errors in the coarse road binary image (some pixels are falsely classified as road or non-road). To detect and correct such errors, a validation procedure based on LRF scan and two

consecutive coarse road binary images is proposed. A LRF is mounted horizontally on the front of the vehicle (see Fig.4(a)), and we suppose that the extrinsic parameters between the LRF and the fisheye camera are known. The laser scan plane is almost parallel to the road surface. So if an object is detected in the laser scan and the corresponding pixels are labeled as road in the coarse road binary image, the validation step considers that an error occurs. However, this condition is not sufficient if we consider the case corresponding to pixels that are falsely classified as non-road. To deal with this case, two consecutive coarse road binary frames are used. Suppose F_k is the current coarse road binary image, and F_{k-1} was the previous one. By experimentation, we find that the amount of road pixels should remain relatively stable between two consecutive frames. So if there exists dramatic change in the amount of road pixels between two consecutive frames, the validation step judges that there is an error in the computed coarse road binary image. In summary about the above two cases, if one of the following conditions is satisfied, an error is suspected, and the refined procedure based on Lab space image will be applied:

$$\begin{cases} P_{LRF} \in P_r \\ M_{F_k} > (1+\beta) M_{F_{k-1}} \\ M_{F_k} < (1-\beta) M_{F_{k-1}} \end{cases} \tag{2}$$

where P_{LRF} denotes a pixel in the coarse road binary image which corresponds to a detected point in the LRF scan, P_r represents the set of road pixels in the coarse road binary image, M_{F_k} and $M_{F_{k-1}}$ are the amounts of the road pixels in F_k and F_{k-1} respectively. β is a threshold set manually. In experiments, it is set to 0.1.

3.2 Refined Road Detection Procedure

The refined procedure uses two consecutive coarse road binary images as inputs to compute the "common image " and the "difference image". Common image and difference image are the images that contain respectively the overlapping road parts and the different road parts of the two consecutive coarse road binary images. The pixels classified falsely in the current coarse road binary image are included in the difference image. So, our objective is to correct the false pixels using the difference image. Firstly, the difference image and the road area S_r are combined to extract the regions of interest (ROI) in the fisheye image which contains the S_r area and the pixels that are classified differently in the two consecutive coarse road binary images. The ROI in the fisheye image is then converted from RGB space to Lab space to form the distance image. The distance image will permit to correct the falsely classified pixels. At last, a combination operation is implemented to form a refined road binary image. The framework of the refined procedure is shown in Fig.2.

Distance Image Computation: The distance image is based on Euclidean metric adopted in Lab space. In Lab color space, the average value of a chosen

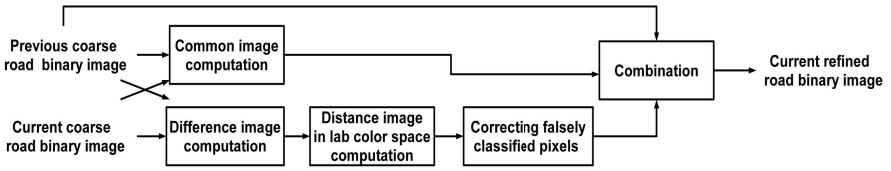

Fig. 2. Framework of refined procedure

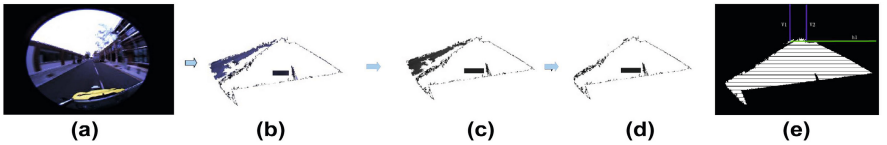

Fig. 3. (a) Original fisheye image (b) The ROI extracted from fisheye image (c) The distance image of the ROI (d) The image I_s (e) The image I_n divided in 17 equal intervals

reference area is computed and the distance between the pixels and this average is calculated. Choosing the reference area is one of the key aspect when applying the metric. In this paper, the road area S_r (already defined in coarse road detection step) is adopted as reference area. The distance image is computed only for ROI of the fisheye image. So, firstly, it is needed to filter the fisheye image to extract these ROI. Let P_i represents the i-th pixel of the fisheye image, S_{sr} denote the set of the pixels of area S_r and V_{Pi} denotes the value of P_i in the binary difference image. The pixel of the fisheye image that satisfies any one of following the two conditions are considered to be pixel of the ROI:

$$\begin{cases} V_{Pi} = 1 \\ P_i \in S_{sr} \end{cases} i = (1, 2, ..., N) \tag{3}$$

As illustrated in Fig.3(b), through this step, most of irrelevant pixels in the original image are discarded. Then, the ROI image is converted from RGB space to Lab space. Let (I_{ls}, I_{as}, I_{bs}) denote the average value of S_r region in L,a,b channels respectively. The distance image (see Fig.3(c)) is defined as follows:

$$d_{lab} = \sqrt{(I_l - I_{ls})^2 + (I_a - I_{as})^2 + (I_b - I_{bs})^2} \tag{4}$$

where I_l, I_a and I_b are the pixel Lab values. The pixel value in the distance image represents the difference between itself and the average value of the road area in Lab color space. It will help us to correct the falsely classified pixels easily.

Correcting Falsely Classified Pixels: In the distance image, a classification operation depending of the S_r area is implemented. Firstly, a pixel is checked if its location is in the range of the road profile of the previous coarse road binary image. The road profile is the outboard edge of the road area in the

coarse road binary image. It seems it is not very exact to employ the road profile of the previous coarse road binary image to represent the current one. However, we actually find that there is no drastic change of road profile between two consecutive frames. The side effect caused by the difference of road profile of two consecutive frames can be reduced by extending the road profile of the previous frame to both sides in horizontal direction. The width of the extension is configured as 10 pixels (experimental data) which can reduce the side effect well. If a pixel is located in the range of road profile and its value is less than a predetermined upper limit threshold T_1, it is reserved as road. Similarly, if the pixel is outside the range and its value is less than a predetermined upper limit threshold T_2, it is also reserved as road. In other cases, the pixel is abandoned. The thresholds $T1$ and T_2 are based on the average value M_{sr} and standard deviation std_{sr} of S_r area in the distance image. Then we have:

$$T = M_{sr} + \alpha * std_{sr} \tag{5}$$

where α is a parameter whose physical meaning is: how much difference is tolerated between the pixel and the reference area in the distance image. For T_1, α is set to 6.5, and for T_2, α is set to 1. Finally, a new image denoted as I_s (see Fig.3(d)) is obtained.

Combination: After I_s is computed, it is added to common image to form a new image I_n. I_n is then divided into K equal intervals according to the height of road area (see Fig.3(e)), and the first interval is scanned. Let h_1 (green line in Fig.3(e)) be the row which corresponds to the lower limit of road area in the first interval, V_1 and V_2 (blue lines in Fig.3(e)) are the columns which correspond to the left and right limits of road area in the first interval respectively. Let L_{ri} and L_{ci} represent the row and column of i-th pixel of the current coarse road binary image respectively. In the coarse road binary image, a road pixel is added to I_n if its location satisfies the following two conditions: .

$$\begin{cases} V_1 < L_{ci} < V_2 \\ L_{ri} < h_1 \end{cases} (i = 1, 2...N) \tag{6}$$

At last, the connect-component algorithm is applied again to remove the pixels which are not connected to road and forms the current refined road binary image.

4 Experimentation

4.1 Set Up

In the experiment, the image sequence is captured by a fisheye camera. The used Fujinon fisheye lens provides up to 185 degrees wide angle. The PL-B742 camera provides 1.3 megapixel (1280×1024) RGB image. The fish-eye camera is mounted on the top of the laboratory vehicle to collect and record experimental data in real road scenarios. The frame rate of the video is 15 fps. The used LRF is a LMS211 providing up to 80 meters measurement range. The layout of these devices is shown in Fig.4(a).

4.2 Experiment Results

(a) (b)

Fig. 4. (a) The configuration of the used experimental platform (b) Experimental results. The images of the first row are original images, the second row are results obtained using the approach proposed in paper [6], the third are the results obtained by the proposed method in this paper.

Table 1. Performance of road detection considering method of [6] and proposed approach under three indicators: average accuracy of road detection (Acc), average of type I error rate (Type I) and average of type II error rate (Type II)

	Approach proposed in this paper				Approach proposed in paper [6]		
Sequence (number of images)	Acc	Type I	Type II	N_{image}	Acc	Type I	Type II
1 (56)	0.9309	0.0038	0.0254	12	0.9083	0.0055	0.0281
2 (128)	0.9028	0.0036	0.0532	87	0.8398	0.0062	0.0831
3 (111)	0.9013	0.0067	0.0247	20	0.8943	0.0073	0.0250
4 (41)	0.8594	0.0063	0.0593	13	0.8447	0.0072	0.0611

The experimental data are composed of 336 images from four different sequences, considering different road environments. To reduce the computational time, all images are down sampled to 640 × 512 pixels resolution. The ground truth is labelled manually. The proposed algorithm is compared with the approach proposed in [6] based only on illumination invariant. For quantitative evaluation, three indicators are calculated: 1) Accuracy 2) Type I error rate 3) Type II error rate. The type I error evaluates the cases: when "true road" pixels are incorrectly rejected. The type II error evaluates the cases: when "non-road" pixel is failed to be rejected. The results are shown in Table I. N_{image} denotes the number of images refined in the sequence. We notice that the most significant improvement is obtained for the sequence 2, for which the percentage of refined images is the greater. Meanwhile, it is remarkable that the proposed approach outperforms

the only illuminant-invariant based algorithm for each indicator. Fig.4(b) shows some experimental results obtained by the approach proposed in this paper and approach proposed in paper [6]. For the first example (first column of fig.4(b)), we can note that the pixels falsely classify as road with approach of paper [6] are well classified as non-road with our approach. For the second image (column 2 of fig.4(b)), we remark that the error that the pixels are classified falsely as non-road with method in paper [6] doesn't appear in our outcome. All above results prove that the combination of various information of image can permit to improve road detection.

5 Conclusion

We proposed an efficient algorithm for road detection in outdoor scenarios. The approach combines Lab color space information, illumination invariant image and LRF scan to extract road area. The experimental results show that the combination of various color space information in image and LRF measurements can permit to achieve some improvements for road detection. For further study, we are trying to integrate other color spaces into the algorithm to reach higher accuracy result for road detection.

References

1. Vandapel, N., Huber, D., Kapuria, A., Hebert, M.: Natural terrain classification using 3-d ladar data. In: IEEE International Conference on Robotics and Automation, vol. 5, pp. 5117–5122 (2004)
2. Douillard, B., Underwood, J., Kuntz, N., Vlaskine, V., Quadros, A., Morton, P., Frenkel, A.: On the segmentation of 3D LIDAR point clouds. In: IEEE International Conference on Robotics and Automation, pp. 2798–2805 (2011)
3. Gallup, D., Frahm, J.-M., Pollefeys, M.: Piecewise planar and non-planar stereo for urban scene reconstruction. In: IEEE Conference on Computer Vision and Pattern Recognition, pp. 1418–1425 (2010)
4. Soquet, N., Aubert, D., Hautiere, N.: Road segmentation supervised by an extended v-disparity algorithm for autonomous navigation. In: IEEE Intelligent Vehicles Symposium, pp. 160–165 (2007)
5. Dahlkamp, H., Kaehler, A., Stavens, D., Thrun, S., Bradski, G.R.: Self-supervised Monocular Road Detection in Desert Terrain. In: Robotics: Science and Systems (2006)
6. Alvarez, J., Lopez, A.: Road detection based on illuminant invariance. IEEE Transactions on Intelligent Transportation Systems 12(1) (2011)
7. Rotaru, C., Graf, T., Zhang, J.: Color image segmentation in HSI space for automotive applications. Journal of Real-Time Image Processing 3(4), 311–322 (2008)
8. Chen, H.-C., Chien, W.-J., Wang, S.-J.: Contrast-based color image segmentation. Signal Processing Letters 11(7), 641–644 (2004)
9. Finlayson, G., Hordley, S., Lu, C., Drew, M.: On the removal of shadows from images. IEEE Transactions on Pattern Analysis and Machine Intelligence 28(1), 59–68 (2006)
10. Tan, C., Hong, T., Chang, T., Shneier, M.: Color model-based real-time learning for road following. In: IEEE Intelligent Transportation Systems Conference, pp. 939–944 (2006)